Journal of Zhejiang University-SCIENCE B (Biomedicine & Biotechnology) 2024 25(12):1071-1082
www.jzus.zju.edu.cn; www.springer.com/journal/11585
E-mail: jzus_b@zju.edu.cn

Research Article
https://doi.org/10.1631/jzus.B2400081

Check for updates

Deciphering odontogenic myxoma: the role of copy number variations as diagnostic signatures

Aobo ZHANG[1,2], Jianyun ZHANG[1,2], Xuefen LI[2,4], Xia ZHOU[3], Yanrui FENG[2,4], Lijing ZHU[1,2], Heyu ZHANG[2,4]✉, Lisha SUN[2,4]✉, Tiejun LI[1,2]✉

[1]*Department of Oral Pathology, Peking University School and Hospital of Stomatology / National Center of Stomatology / National Clinical Research Center for Oral Diseases / National Engineering Research Center of Oral Biomaterials and Digital Medical Devices, Beijing 100081, China*
[2]*Research Unit of Precision Pathologic Diagnosis in Tumors of the Oral and Maxillofacial Regions, Chinese Academy of Medical Sciences (2019RU034), Beijing 100081, China*
[3]*Department of Oral and Maxillofacial Surgery, Peking University School and Hospital of Stomatology, Beijing 100081, China*
[4]*Central Laboratory, Peking University School and Hospital of Stomatology, Beijing 100081, China*

Abstract: In light of the lack of reliable molecular markers for odontogenic myxoma (OM), the detection of copy number variation (CNV) may present a more objective method for assessing ambiguous cases. In this study, we employed multiregional microdissection sequencing to integrate morphological features with genomic profiling. This allowed us to reveal the CNV profiles of OM and compare them with dental papilla (DP), dental follicle (DF), and odontogenic fibroma (OF) tissues. We identified a distinct and robustly consistent CNV pattern in 93.75% (30/32) of OM cases, characterized by CNV gain events in chromosomes 4, 5, 8, 10, 12, 16, 17, 20, and 21. This pattern significantly differed from the CNV patterns observed in DP, DF, and OF. The Kyoto Encyclopedia of Genes and Genomes (KEGG) analysis indicated potential links between this CNV patterns and the calcium signaling pathway and salivary secretion, while Gene Ontology (GO) term analysis implicated CNV patterns in tumor adhesion, tooth development, and cell proliferation. Comprehensive CNV analysis accurately identified a case that was initially disputable between OF and OM as OM. Our findings provide a reliable diagnostic clue and fresh insights into the molecular biological mechanism underlying OM.

Key words: Odontogenic myxoma; Copy number variation; Odontogenic fibroma; Odontogenic fibromyxoma; Diagnostic marker

1 Introduction

The histology of odontogenic myxoma (OM), a rare benign neoplasm characterized by sparse spindle or stellate cells embedded in a myxoid extracellular matrix, resembles that of odontogenic ectomesenchyme. As the third most frequent type of odontogenic tumor (Mete and Wenig, 2022), OM demonstrates an aggressive proclivity for infiltrating adjacent tissues and recurring post surgical excision (Li et al., 2006). Consequently, extensive resection is required (Kawase-Koga et al., 2014; Kauke et al., 2018), potentially causing substantial damage to the surrounding normal tissues. OM primarily affects young adults in their second or third decades of life (Francisco et al., 2017), so the need for an innovative and conservative therapy to maintain the quality of life post treatment is pressing. However, our understanding of the underlying mechanisms of OM remains limited (Gomes et al., 2011; Santos et al., 2017).

Moreover, since Thoma and Goldman's initial report of jaw myxoma in 1947 (Thoma and Goldman, 1947), no comprehensive studies analyzing the best practices for OM diagnosis have been published. Differential diagnosis for dental papilla (DP) and dental

✉ Tiejun LI, litiejun22@vip.sina.com
Lisha SUN, lisa_sun@bjmu.edu.cn
Heyu ZHANG, zhangheyu1983@sina.cn
Tiejun LI, https://orcid.org/0000-0001-5983-2985
Lisha SUN, https://orcid.org/0000-0002-4571-3739
Heyu ZHANG, https://orcid.org/0000-0002-4461-2290
Aobo ZHANG, https://orcid.org/0000-0003-0568-8601

Received Feb. 14, 2024; Revision accepted July 10, 2024; Crosschecked Nov. 22, 2024

follicle (DF) (Suarez et al., 1996), both of which originate from odontogenic ectomesenchyme, was emphasized in World Health Organization (WHO)'s 2022 report (Mete et al., 2022). Distinguishing between OM and odontogenic fibroma (OF) also presents a clinical challenge due to their overlapping histopathology and similar clinical presentation. Comprehensive diagnostic approaches, including clinical, radiographic, and histopathological evaluations, are often needed (Alhousami et al., 2018) and, in some cases, must be supplemented by molecular genetic analyses. This precision is crucial, as OF usually warrants a more conservative surgical approach, while OM often necessitates broader surgical resection due to its recurrent, infiltrative nature. Therefore, addressing these issues in OM diagnosis and understanding its molecular mechanisms are of utmost importance.

Copy number variation (CNV) is a major type of DNA structural variation that involves genomic rearrangement, including amplifications (gains) and deletions (losses) that affect the integer copy numbers of various portions of the genome (Mikhail, 2014; Lauer and Gresham, 2019; Zhong et al., 2021). Many CNV events have been implicated in various diseases, including cancers, neurodegenerative diseases, and metabolic diseases (Cooper et al., 2011; Almal and Padh, 2012; Zhan et al., 2020). Recent studies have suggested CNV's potential utility in the differential diagnosis and risk assessment of oral tumors (Li et al., 2021; Ma et al., 2021; Cai et al., 2023). Moreover, CNV can impact gene expression and serve as a therapeutic target in some diseases (Stranger et al., 2007; Tang and Amon, 2013; Lyu et al., 2022).

In this study, we aimed to utilize CNV profiling to enhance OM diagnosis and preliminarily explore its molecular mechanisms. We employed laser-capture microdissection (LCM) to precisely capture the morphology with CNV profiling in OM, DP, DF, and OF. Through bioinformatics analysis, we sought to identify CNV differences between the diseases and explore potential molecular mechanisms underlying OM.

2 Materials and methods

2.1 Sample collection and preparation

We collected tissue samples from the Peking University School and Hospital of Stomatology, including 32 OM samples (18 fresh-frozen, 14 paraffin-embedded; Table S1), 10 OF samples (all paraffin embedded; Table S2), and samples from four young patients who required immature tooth extraction due to orthodontic indications (all fresh-frozen; Table S3, Fig. S1b). Diagnoses were facilitated by considering histopathologic criteria in accordance with the 2022 version of the WHO Classification of Head and Neck Tumors (fifth edition) (Mete et al., 2022). We gathered and analyzed the clinical data of all incorporated cases, which were reviewed and validated by three experienced pathologists. All specimens were sectioned into 10-μm tissue slices and placed on enzyme-treated polyethylene naphthalate (PEN) membrane slides that were free of DNA/RNA.

For formalin-fixed paraffin-embedding (FFPE) specimens, tissue slides underwent three 10-min soaking cycles in dimethylbenzene, followed by a rehydration sequence involving 1-min ethanol immersion (concentrations (volume fraction): twice at 100%, then 90%, 80%, and finally 70%). After washing the slides with diethyl pyrocarbonate (DEPC) water, we performed hematoxylin and eosin (H&E) staining following a standard protocol. Dehydration was executed with a series of ethanol solutions (70%, 80%, 90%, and 100% ethanol). For optimal cutting temperature (OCT) compound-embedded fresh-frozen samples, tissue slides were briefly immersed in 70% ethanol, and H&E staining was performed after DEPC water washing. The dehydration protocol was identical to that for FFPE samples. All slides were then digitally scanned using a Nano Zoomer Digital scanner (Hamamatsu, Japan) (Fig. 1a).

2.2 Laser-capture microsection and DNA sequencing

We utilized laser microdissector (LMD7, Leica, Germany) to microdissect the H&E-stained slides (Fig. 1b). Areas corresponding to OM, adjacent normal bone, DP, DF, and OF were identified, captured, and independently vetted by three independent, experienced pathologists. The captured tissues (300–500 cells) were lysed in 10 μL of lysis buffer (0.10 μL of total transcriptome RNA extraction (TTE) Mix V50 (Vazyme, Nanjing, China), 0.25 μL of 50× proteinase inhibitor (Promega, Madison, USA), 4.00 μL of 5× tagment DNA (TD) buffer, 0.20 μL of 0.10 mol/L $MgCl_2$, and 5.45 μL of nuclease-free water) at 50 °C for 12 h to obtain DNA. Then, the DNA underwent tagmentation by Tn5-transposase (TD501-02, Vazyme) (Fig. 1c) at 55 °C for 2 h and amplification in a reaction mixture

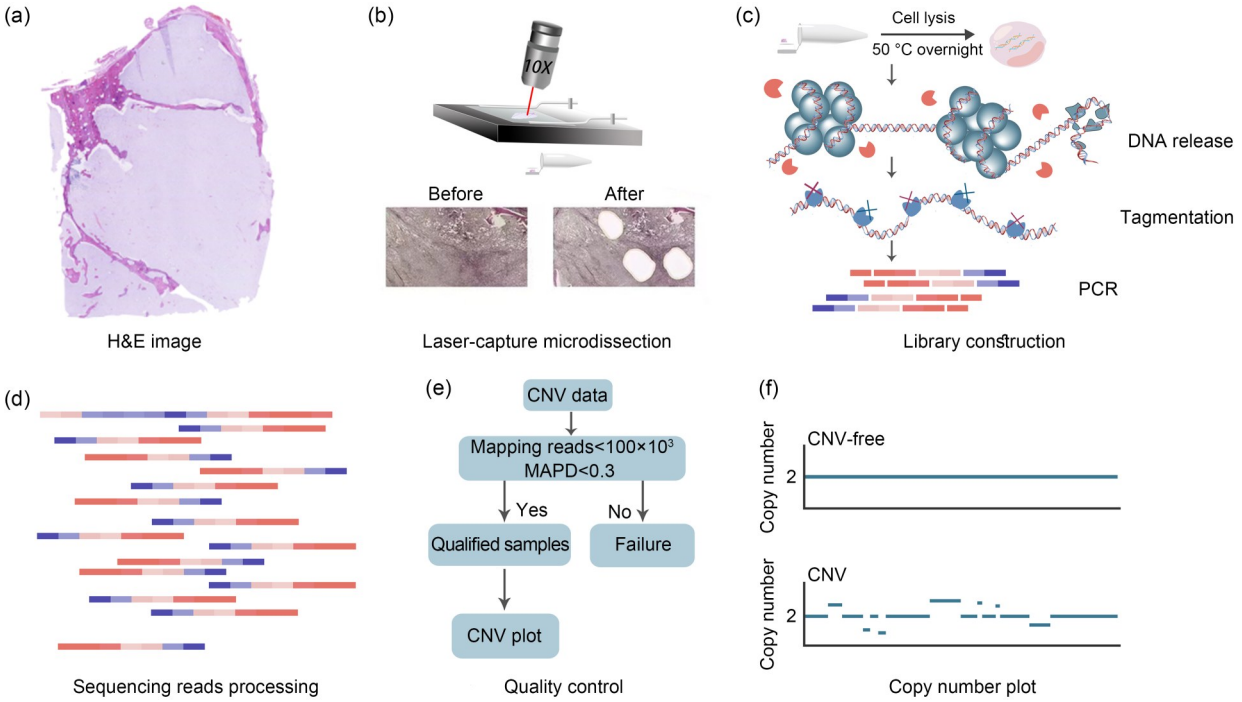

Fig. 1 Workflow of the multiregional microdissection sequencing (MMS) approach. (a) Hematoxylin and eosin (H&E) staining was performed on tissue sections, each measuring 10 μm in thickness. (b) Utilizing laser-capture microdissection (LCM), 300–500 cells were isolated from 10-μm sections and then subjected to lysis buffer. (c) Construction of sequencing libraries was facilitated by Tn5-transposase, wherein DNA molecules were tagmented, barcoded, and subsequently polymerase chain reaction (PCR)-amplified. (d) Next-generation sequencing reads underwent mapping to the reference genome and subsequent quantification to deduce the copy-number ratio. (e) Samples exhibiting low quality were excluded based on criteria involving amplification noise and mapped reads. (f) Subsequent analysis utilized samples irrespective of the presence or absence of copy number variations (CNVs). CNV-free: no significant CNV events occurred.

(22 μL Q5 High-Fidelity 2× Master Mix (New England Biolabs, Massachusetts, USA), 1 μL 10 mmol/L Nextera i5 primer, 1 μL 10 mmol/L Nextera i7 primer, and 10 μL tagmentation template) by 25 cycles of polymerase chain reaction (PCR) and purification using clean DNA beads (VAHTS, Vazyme). Approximately 2 μg of DNA library product was obtained for each sample, the concentration of each sample was measured using a Qubit system (Invitrogen, California, USA), and the fragment size was determined using a fragment analyzer (Agilent, California, USA). The typical size ranged from 300 to 700 bp. Finally, the DNA library product was sequenced using the Illumina HiSeq 4000 sequencer (Illumina, California, USA) with PE150. The segment-level CNV was acquired, with each bulk sample having a sequencing average size of 0.3 Gb (0.1×).

2.3 Bioinformatics and statistical analysis

After obtaining DNA sequence data, we used Cutadapt (version 2.10) to trim the adapter sequence from the data (Kechin et al., 2017) and aligned the reads to the human genome 19 (hg19) assembly via Bowtie2 aligner (version 2.2.9) (Langmead and Salzberg, 2012) (Fig. 1d); 1 mol/L mapped reads were obtained from each sample. Before initiating bioinformatic analysis, the primary threshold was applied to further exclude unqualified sequencing data, requiring a median absolute pairwise difference (MAPD) below 0.30 and a number of mapped reads exceeding 100 000. This resulted in the removal of 128 unqualified samples, leaving a total of 318 samples for analysis (Figs. 1e and 1f). The copy number was obtained via the DNAcopy package (version 1.64.0) in R, using the circular binary segmentation (CBS) algorithm (min.width=5, alpha=0.1, undo.SD=0.1) (Langmead and Salzberg, 2012).

For diploid chromosomes, copy-number gain was defined as copy number>2.4, and copy-number loss was defined as copy number<1.7. For haploid chromosomes, copy-number gain was defined as copy number >1.5, and loss was defined as copy number<0.5 (Li

et al., 2021; Ma et al., 2021). The CNV score was used to quantify the complexity of CNV. The CNV score is calculated by

$$\text{CNV score} = \sum_{\text{chr}=1}^{24}(\text{mean}(|s_i - s_{i-1}|) + |\text{mean}(s_i) - \text{norm}|),$$

where i is the sequence number of the position of the genome and norm is the neutral copy number per segment (norm=0, 1, or 2).

After calling the copy number for each sample, we performed a series of CNV analyses, including gene annotation (the gene list for hg19 was downloaded from GENCODE; https://www.gencodegenes.org/human/release_19.html), establishing the matrix (gene name and sample name), screening the genes identified by Chi-square test, and performing Kyoto Encyclopedia of Genes and Genomes (KEGG) and Gene Ontology (GO) functional analyses of these screened genes.

In conducting the specific GO and KEGG analyses, our initial step entailed mapping the CNV genes to each respective term in the GO and KEGG databases, followed by enumerating the genes associated with each term. Subsequently, we utilized the hypergeometric distribution test, with the GO and KEGG annotation status of the entire genome as background, to identify significantly enriched GO and KEGG terms for CNV genes (P<0.01). These analyses utilized the R packages "clusterprofiler," "org.Hs.cg.db," "enrichplot," and "ggplot2."

All statistical analyses were carried out in either Python version 3.8.5 (mainly used for data text processing) or R version 4.2.1. (mainly used for data analysis and generating visualization results). P<0.01 was deemed statistically significant.

3 Results

3.1 Clinicopathological findings on OF and OM

Tables S1 and S2 detail the clinical characteristics of the 42 cases included in this study, 32 of which were OM and 10 of which were OF. Among the 32 OM cases, 12 occurred in the maxilla (MA) and 20 occurred in the mandible (MB). The male-to-female ratio was 1:1.29 (male 14, female 18), and the age at admission/hospitalization was (33.03±14.89) years (ranging from 1 to 73 years). Disease duration was (11.34±14.55) months (ranging from 0.04 to 6.00 years). Among the ten OF cases, five occurred in the MA, and five in the MB. The male-to-female ratio was 4:1 (male 8, female 2), and the age at admission/hospitalization was (36.00±11.35) years (ranging from 24 to 62 years). Disease duration was (2.17±2.02) years (ranging from 0.2 to 6.0 years). Histologically, OM mainly comprises loosely arranged, stellate, and spindle-shaped cells with abundant mucus and/or abundant collagen fibers (Fig. 2a). Similarly, OF primarily consists of abundant collagen fibers (Fig. 2b). Fig. S1 provides a sample of OM through macroscopic observation and panoramic radiograph.

3.2 Comprehensive CNV analyses of DP, DF, OF, and OM

Upon analyzing the OM cases, we found that the CNV gain events of cells in the myxoid area (Fig. 2a; Area 2: mucoid) primarily occurred on chromosomes 4, 5, 8, 10, 12, 16, 17, 20, and 21. This pattern was significantly different from the adjacent normal bone-tissue cells that demonstrated no CNV events (Fig. 2a; Area 1: bone). In addition, the CNV pattern of cells in the fibrous area was consistent with that of the myxoid tissue area (Fig. 2a; Area 3: fibrous; Area 4: mucoid). For DP, DF, and OF, the CNV patterns were also significantly different from those of OM (Fig. 2b). In particular, DP and DF exhibited virtually no CNV events, and the CNV of OF cells in the abundant collagen area was not as complex as that of OM (Fig. 2b).

To verify these findings, we expanded the sample size for CNV data by repeatedly collecting a minimum of five similar bulk samples per case for each tissue type using multiregional microdissection sequencing (MMS). We then categorized 318 samples which were all from 4 DP, 4 DF, 10 OF, and 32 OM cases into DP/DF (71 samples), OF (75 samples), and OM (172 samples) groups. A heatmap based on chromosome sites and copy numbers was then formed (Fig. 3a). Visually, the CNV pattern of the OM group significantly differed from the other two groups, and within the OM group, the CNV patterns remained remarkably consistent. The specific significant CNV patterns in DP, DF, OF, and OM are summarized in Table 1.

Considering the relatively small proportion of CNV events on some chromosomes, we highlighted the main pattern of CNV occurrence in each group by identifying chromosomes in each group where more than 25% of samples displayed CNV events. As shown in Fig. 3b,

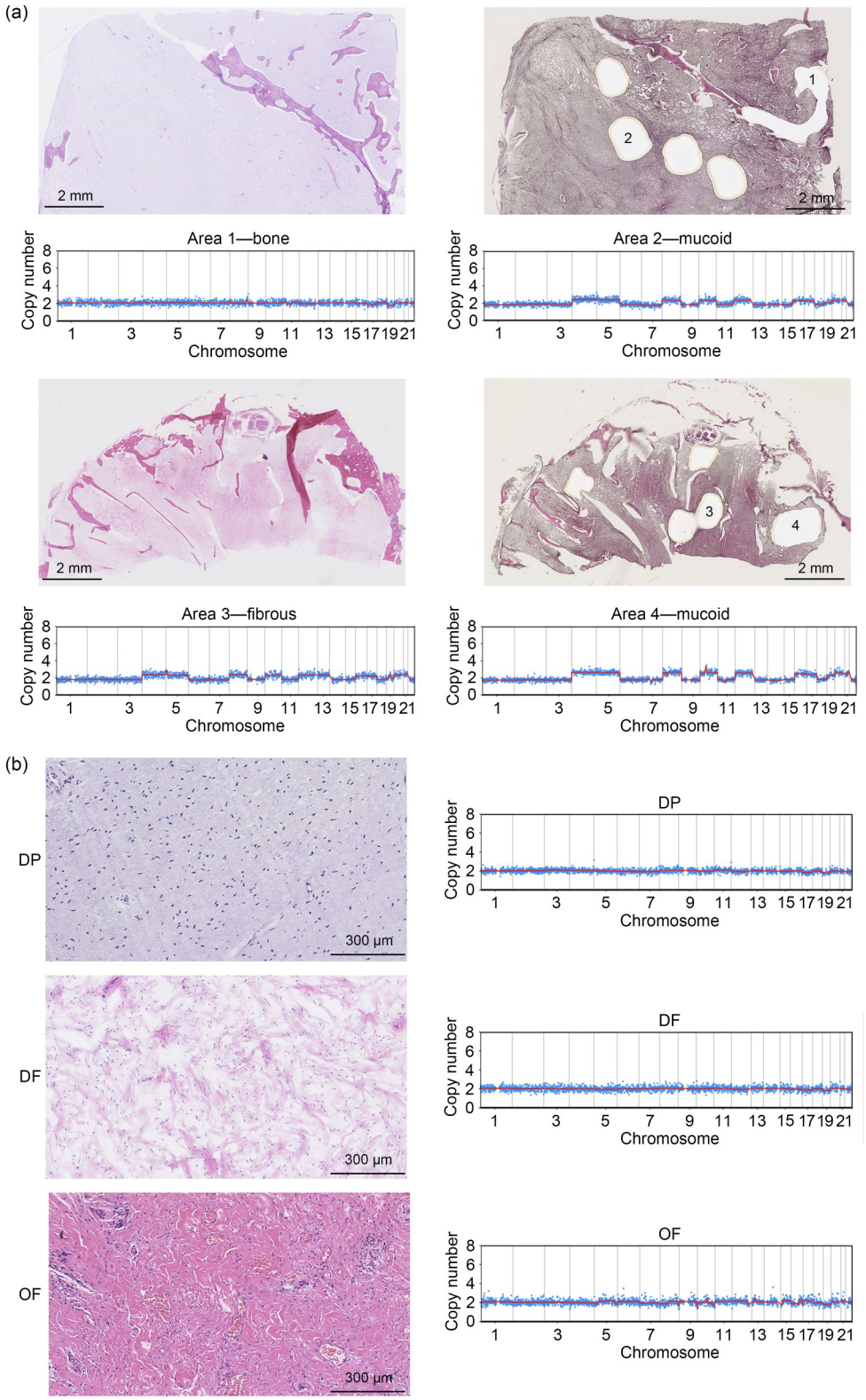

Fig. 2 Copy number variation (CNV) plots for representative odontogenic myxoma (OM), dental papilla (DP), dental follicle (DF), and odontogenic fibroma (OF) samples. (a) Haematoxylin and eosin (H&E) staining images demonstrating OM with corresponding areas subjected to microdissection and their CNV profiles. (b) H&E staining images for DP, DF, and OF with corresponding microdissection areas and their CNV profiles.

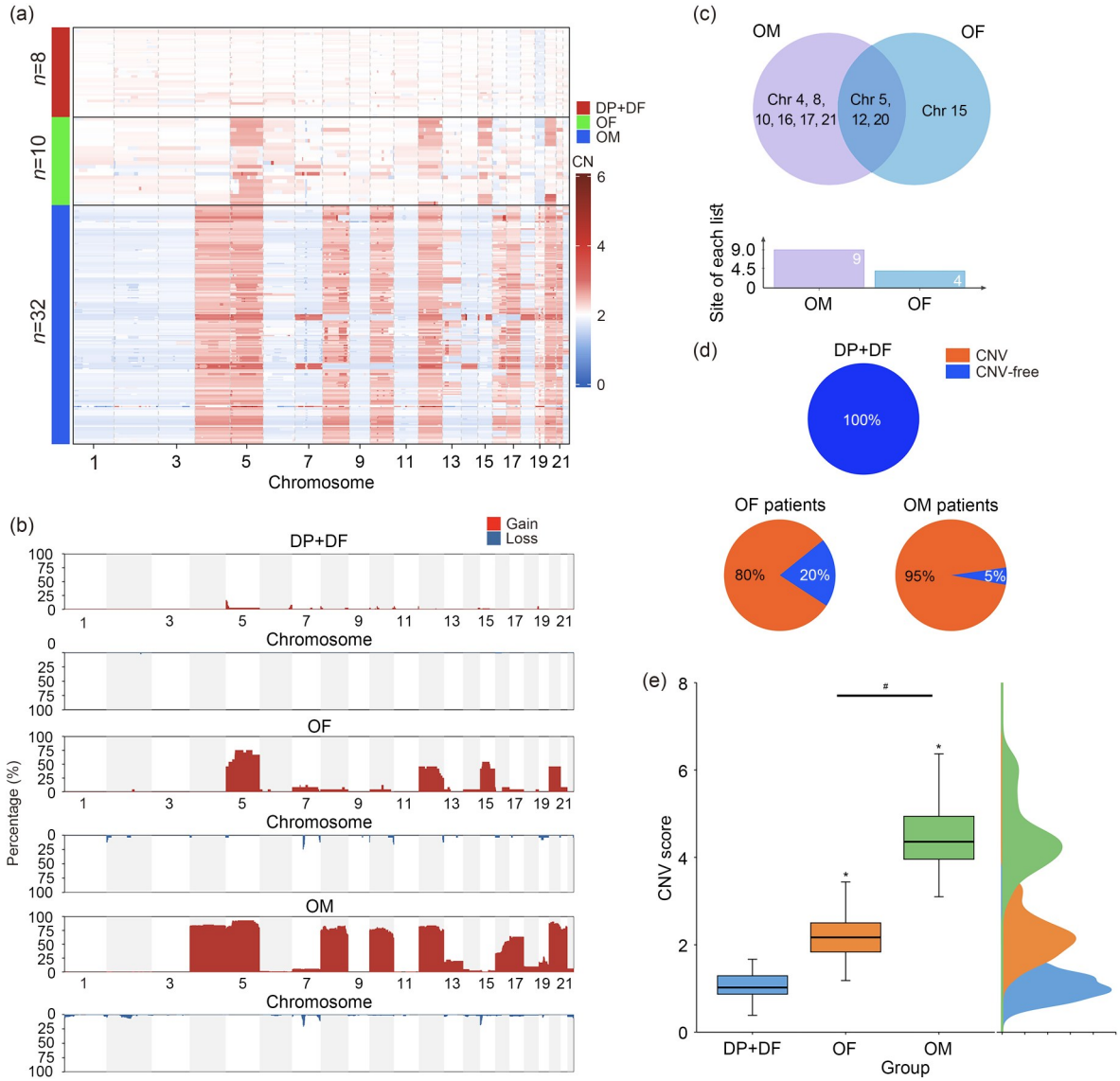

Fig. 3 Comprehensive copy number variation (CNV) analysis of dental papilla (DP), dental follicle (DF), odontogenic fibroma (OF), and odontogenic myxoma (OM). (a) Heatmap presenting CNV landscape of all samples collected. The *x*-axis represents chromosomes, and the *y*-axis shows the group color (red, green, or blue) and the number of patients. The DP+DF group (red) denotes the CNV of four young patients with four DP tissues and four DF tissues, the OF group (green) indicates the CNV of ten patients, and the OM group (blue) represents the CNV of 32 patients, illustrating a highly consistent pattern. Red in copy number (CN) represents CNV gain events, while blue denotes CNV loss events. (b) Bar plot for the DP+DF, OF, and OM groups, indicating the percentage of samples harboring CNV (on the *y*-axis). Red represents CNV gain events, while blue denotes CNV loss events. (c) The Venn diagram displays specific chromosomes harboring CNV events in the OF+OM groups, while the intersecting region represents the shared chromosomes (chr 5, 12, and 20). The unique chromosomes for OM include chr 4, 8, 10, 16, 17, and 21, while the unique chromosome for OF is chr 15, which could be the differential point between OM and OF. Chr: chromosome. (d) Ratio of patients with or without CNV in DP+DF (upper panel), OF (left panel), and OM (right panel). (e) Boxplots with normalized frequency distribution showing the CNV scores. The asterisk (*) denotes a comparison with the DP+DF group, while the hash (#) signifies a comparison between the OF and OM groups. * *P*<0.001, # *P*<0.001.

CNV events did not occur in DP or DF. In contrast, the OF group mainly exhibited "gain" CNV events on chromosomes 5 (percentage of samples harboring CNV=66.89%), 12 (41.97%), 15 (48.14%), and 20 (45.83%). Similarly, OM mainly demonstrated "gain" CNV events across more chromosomes, including

Table 1 Significant CNV patterns identified in OM, DP, DF, and OF

Group	CNV/total case	CNV pattern
OM	30/32	Chr 4, 5, 8, 10, 12, 16, 17, 20, and 21
OF	8/10	Chr 5, 12, 15, and 20
DP+DF	0/4	CNV-free

CNV: copy number variation; OM: odontogenic myxoma; DP: dental papilla; DF: dental follicle; OF: odontogenic fibroma; CNV-free: no significant CNV events occurred; Chr: chromosomes.

chromosomes 4 (84.28%), 5 (89.62%), 8 (79.03%), 10 (76.05%), 12 (76.41%), 16 (44.15%), 17 (63.59%), 20 (87.63%), and 21 (79.12%). Fig. 3c uses a Venn diagram to identify the unique and shared chromosomes between OF and OM that exhibited CNV. Fig. 3d shows that the majority of OM cases (93.75%, 30 out of 32; Table S1) exhibited CNV events, 80% of OF cases (8 out of 10; Table S2) harbored CNV, and all DP and DF cases were CNV-free (Table S3).

To evaluate the CNV pattern more intuitively and accurately, we calculated the CNV scores for the three groups. As Fig. 3e illustrates, the CNV score of the DP/DF group was 1.065±0.299 (ranging from 0.386 to 1.668). The OF group had a significantly larger CNV score of 2.217±0.541 (ranging from 1.181 to 3.438) compared to the DP/DF group (P<0.001). The OM group had the highest CNV score of 4.520±0.796 (ranging from 3.100 to 6.371), which was significantly larger than those of the DP/DF and OF groups, indicating a higher degree of CNV complexity for OM.

3.3 Potential molecular pathways for CNV in OM

GO and KEGG enrichment analyses showed that three biological process terms, three cell-component terms, one molecular function term (Fig. 4b), and two KEGG pathways (Fig. 4a) were significantly enriched (P<0.01), and their corresponding gene lists are given in the Tables S4 and S5. Significantly, both the calcium signaling pathway (CSP) and salivary secretion (SS) from the KEGG pathway category are associated with the generation of mucus, which is the main extracellular matrix component of OM.

3.4 Case study (Case I): differential diagnosis assisted by CNV profiles

In this study, we included one case (Case I, detailed at the bottom of Table S1) in which the diagnosis was suspected to be either OM or OF due to the presence of abundant fibrous tissues (Fig. 5a). This case involved a 13-year-old male patient who was brought to our hospital due to slow progression, as well as spontaneous pain and swelling on the left side of the lower mandible, which was ongoing for one year.

Considering the patient's young age and the family's strong desire to maintain his facial structure for a higher quality of life, the type of surgery required was a matter

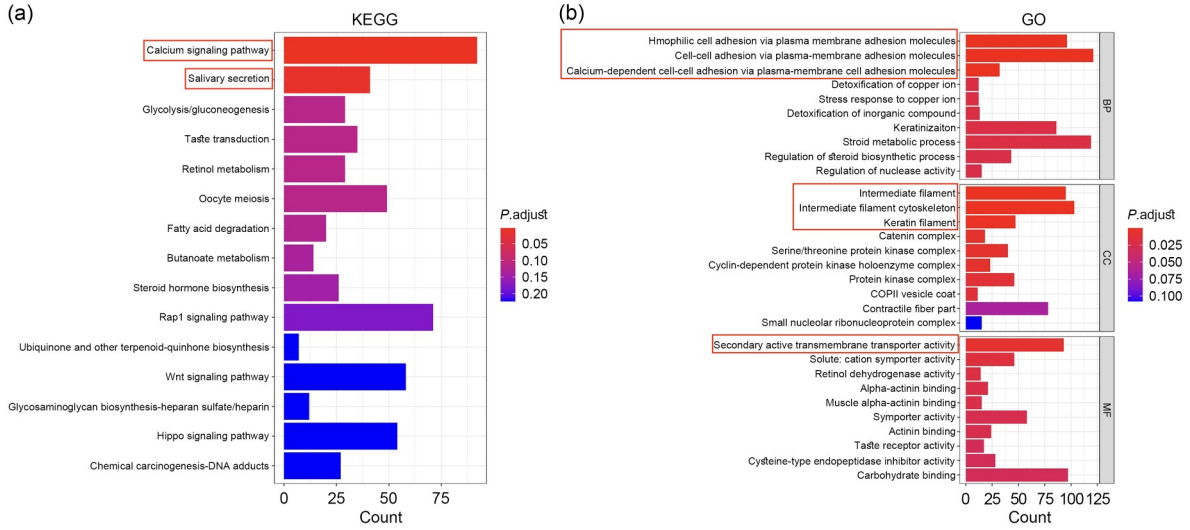

Fig. 4 Potential molecular pathways for copy number variation (CNV) of odontogenic myxoma (OM). Functional enrichment analyses of genes corresponding to CNV of OM visualized by Kyoto Encyclopedia of Genes and Genomes (KEGG) pathways (a) and Gene Ontology (GO) terms (b). The abscissa represents gene counts and the ordinate denotes the name of the KEGG pathway and GO term. The redness of a column signifies a higher degree of enrichment (smaller adjusted *P*-value). *P*adjust: adjusted *P*-value; BP: biological process; CC: cellular component; MF: molecular function.

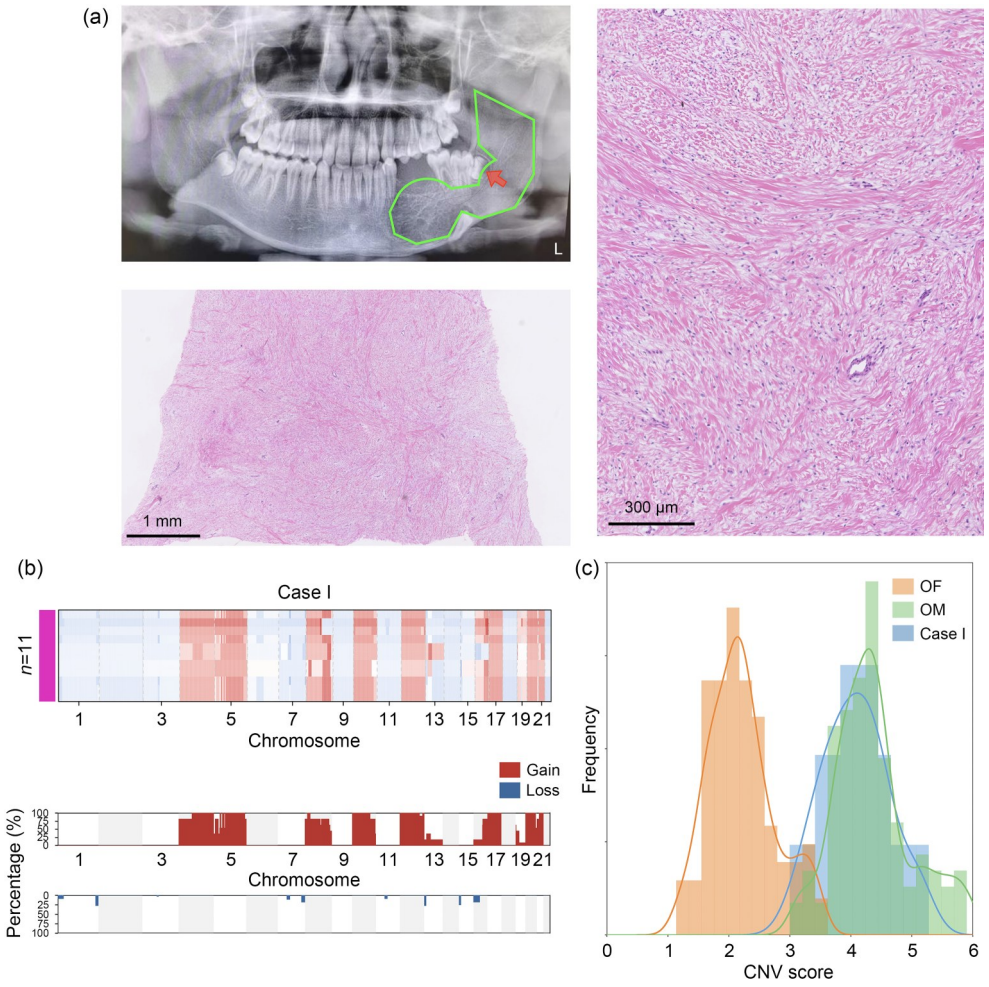

Fig. 5 Differential diagnosis evaluation for a case (Case I): odontogenic fibroma (OF) or odontogenic myxoma (OM)? (a) Panoramic radiograph of Case I illustrating the extent of the lesion's invasion in the left mandible, a characteristic of OM. Green demarcation specifies the lesion's boundary, while a red arrow indicates an immature tooth implicated in the lesion. Haematoxylin and eosin (H&E) staining images show the tissue morphology of Case I. (b) Copy number variation (CNV) profiles of 11 samples from Case I. A heatmap (upper panel) and bar plot (lower panel) show the key CNV events associated with specific chromosomes. For the lower panel, the *y*-axis denotes the percentage of samples harboring CNVs. (c) Normalized frequency distribution of CNV score in Case I and in OF and OM samples.

of utmost importance. A diagnosis of OM would necessitate mandible resection with flap reconstruction, a procedure that could significantly damage the patient's normal tissue. On the other hand, a diagnosis of OF would allow for more conservative surgery.

To accurately determine the characteristics of the CNV pattern, we carried out MMS on 11 samples from this case. The CNV analysis revealed that prominent chromosomes in Case I (4, 5, 8, 10, 12, 16, 17, and 19–21) exhibited CNV gain events (Fig. 5b), consistent with the pattern seen in OM. Notably, these samples lacked CNV events on chromosome 15, which is uniquely observed in OF. Furthermore, the CNV score of Case I (4.08±0.54) aligned with that of OM (Fig. 5c).

Radiographic evidence showed that the lesion extended across the entire mandibular body (Fig. 5a) and involved an impacted tooth (red arrow), suggesting local invasion within the jaw. Based on these findings, the case was more appropriately classified as OM rather than OF. This diagnostic clarification influenced the surgical approach, leading the team to perform an expanded resection to mitigate the risk of recurrence.

4 Discussion

The genetic basis of OM is not fully understood, with studies examining the positive mutations on

genomics within OM being notably limited. A 2017 research effort employed next-generation sequencing to explore potential mutations in 50 common tumor genes within OM; however, no pathogenic mutations were identified (Santos et al., 2017). In addition, the type 1α regulatory subunit (RIα) of cyclic adenosine monophosphate (cAMP)-dependent protein kinase (PKA) (PRKAR1A) has been proved to play a role in the development of cardiac myxomas (Maleszewski et al., 2014), but one study found that only 2 of 17 OM cases showed mutations in the *PRKAR1A* gene (Best-Rocha et al., 2016). The chromosomal structural variation within OM, however, remains relatively unexplored.

Next-generation sequencing (NGS) represents a potent methodology for scrutinizing the composition and functionality of tissues (Chen et al., 2023). In this study, we used MMS to characterize the CNV pattern of OM and found that most OM cases (93.75%) had an extremely consistent and unique CNV pattern. The validity of this pattern required verification with strict control groups. Accordingly, we compared CNV of OM with adjacent normal bone tissue, considering OM's primary manifestation in the jawbones. The adjacent bone tissue exhibited almost no CNV events, emphasizing the distinct nature of the CNV pattern of OM.

However, bone tissue is not mesenchymal tissue, and the DP and DF, which are mesenchymal portions of the tooth germ, are the recognized sources of OM histogenesis (Gomes et al., 2011). OM's propensity to invade or incorporate the tooth germ, particularly in young patients (Chrcanovic and Gomez, 2019), emphasizes the criticality of differentiating between the tooth germ and OM to avoid injuring the tooth germ. Our findings revealed that DP and DF also exhibited virtually no CNV events, marking a significant difference from OM. In addition, we found that the CNV patterns of cells in the fibrous and myxoid areas were identical, indicating that they were the same clones. Interestingly, based on our previous research regarding CNV on fibrous dysplasia (FD) (Ma et al., 2021), we found that the CNV of OM was also completely different from that of FD, which further solidified the concept that the CNV pattern of OM is an inherent characteristic of the disease.

Given the consistency of CNV in OM, probing its underlying mechanism might provide valuable insights. By analyzing the genetic information associated with CNV in OM, we discovered that the CSP and SS are implicated in KEGG. The CSP, under aberrant conditions, can modulate critical aspects of tumor progression, such as tumor proliferation (Hao et al., 2015), evasion from cell death (Legrand et al., 2001), and autophagy in cancer (Samuel et al., 2018), and numerous anticancer therapies target the CSP (Williams et al., 2013). Notably, CSP is also involved in SS, which might explain the abundant mucoid matrix morphology in OM. GO analysis demonstrated that the related pathways were mainly involved in the adhesion of tumors, which is potentially linked to the mucous extracellular matrix environment in OM, tooth development, and cell proliferation. In particular, the GO term "intermediate filament" has been detected in the OM, with nestin, an intermediate filament, being detected in OM cases (Fujita et al., 2006).

Odontogenic fibromyxoma (OFM) is a term used to describe OM cases that present with substantial amounts of collagen (Regezi et al., 2015). These cases could be easily confounded with OF, as both tumors contain fibrous collagen. However, the management strategies for OF and OM differ significantly: OF presents with few recurrences and no malignant transformations, whereas OM frequently exhibits local invasion, easy recurrence, and a potential for malignant transformation into odontogenic myxosarcoma (Pahl et al., 2000). Therefore, it is of utmost importance to distinguish between OF and OM objectively and accurately to aid clinicians in deciding on the most appropriate treatment (Haser et al., 2016). In this study, we analyzed the CNV patterns of ten OF cases and found them to be significantly different from those of OM. We also identified a case with an ambiguous diagnosis, which was confirmed to be OM through CNV analysis, underscoring the potential diagnostic utility of CNV analysis in such cases.

5 Limitations

To fully understand the significance of the unique and consistent CNV pattern observed in OM, further research is warranted. Our study was based on genomic data, and since CNV can affect gene expression (Stranger et al., 2007), it would be beneficial to complement our findings with transcriptomic studies and identification of potential driving genes through immunohistochemistry or immunofluorescence techniques. Additionally,

as OM is a rare disease, the number of cases included in this study was limited. Thus, it is possible that there are other CNV patterns that have not been identified yet. To confirm the presence of a unique CNV pattern in OM, further research involving more cases, possibly obtained through multicenter studies, is necessary.

6 Potential for clinical application

Since there is currently no reliable molecular marker for OM, including immunohistochemistry (IHC) markers and mutation or fusion genes, CNV detection may offer a more objective evaluation method for ambiguous cases. In addition, the MMS approach allows for the extraction of a minimal amount of viable DNA, ensuring reliable sequencing data for high-resolution CNV analysis. In this study, we identified a consistent and unique CNV pattern via MMS. The sequencing depth for CNV (a mere 0.3 Gb) substantially reduces costs, potentially making clinical application more convenient and efficient. Therefore, we believe that the CNV acquired through the MMS approach warrants consideration for regular diagnostic application, given the inadequacy of conventional pathology techniques in achieving precise OM diagnosis. The prospective diagnostic framework for OM could utilize a CNV pattern via MMS to enhance diagnostic precision when clinicians encounter histopathological overlap of OM with other jaw lesions.

7 Conclusions

This study is the first to identify a unique and consistent CNV profile in OM, providing a valuable foundation for differential diagnosis and a path for research into the molecular mechanisms underpinning OM.

Data availability statement

The authors declare that the data supporting the findings of this study are available within the paper and its supplementary information files. Should any raw data files be needed in another format, they are available from the corresponding author upon reasonable request.

Acknowledgments

This work was supported by the National Natural Science Foundation of China (Nos. 81671006 and 81300894), the CAMS Innovation Fund for Medical Sciences (No. 2019-I2M-5-038), and the Program for New Clinical Techniques and Therapies of Peking University Hospital of Stomatology (No. PKUSSNCT-22A14), China.

Author contributions

Aobo ZHANG performed the experimental research and data analysis, and wrote and edited the manuscript. Jianyun ZHANG, Xia ZHOU, and Lijing ZHU contributed to conception, data acquisition and interpretation, and drafted the manuscript. Xuefen LI and Yanrui FENG contributed to data acquisition and interpretation. Tiejun LI, Lisha SUN, and Heyu ZHANG contributed to conception and design, and critically revised the manuscript. All authors have read and approved the final manuscript, and therefore, have full access to all the data in the study and take responsibility for the integrity and security of the data.

Compliance with ethics guidelines

Aobo ZHANG, Jianyun ZHANG, Xuefen LI, Xia ZHOU, Yanrui FENG, Lijing ZHU, Heyu ZHANG, Lisha SUN, and Tiejun LI declare that there are no conflicts of interest in the study.

All procedures involving human tissues were approved by the Institutional Review Board of Peking University Hospital of Stomatology (Approval No. PKUSSIRB-202385024).

References

Alhousami T, Sabharwal A, Gupta S, et al., 2018. Fibromyxoma of the jaw: case report and review of the literature. *Head Neck Pathol*, 12(1):44-51. https://doi.org/10.1007/s12105-017-0823-0

Almal SH, Padh H, 2012. Implications of gene copy-number variation in health and diseases. *J Hum Genet*, 57(1):6-13. https://doi.org/10.1038/jhg.2011.108

Best-Rocha A, Patel K, Hicks J, et al., 2016. Novel association of odontogenic myxoma with constitutional chromosomal 1q21 microduplication: case report and review of the literature. *Pediatr Dev Pathol*, 19(2):139-145. https://doi.org/10.2350/15-05-1637-cr.1

Cai XJ, Zhang JY, Zhang HY, et al., 2023. Biomarkers of malignant transformation in oral leukoplakia: from bench to bedside. *J Zhejiang Univ-Sci B (Biomed & Biotechnol)*, 24(10):868-882. https://doi.org/10.1631/jzus.B2200589

Chen QM, Wang YH, Shuai J, 2023. Current status and future prospects of stomatology research. *J Zhejiang Univ-Sci B (Biomed & Biotechnol)*, 24(10):853-867. https://doi.org/10.1631/jzus.B2200702

Chrcanovic BR, Gomez RS, 2019. Odontogenic myxoma: an updated analysis of 1,692 cases reported in the literature. *Oral Dis*, 25(3):676-683. https://doi.org/10.1111/odi.12875

Cooper GM, Coe BP, Girirajan S, et al., 2011. A copy number variation morbidity map of developmental delay. *Nat Genet*,

43(9):838-846.
https://doi.org/10.1038/ng.909

Francisco ALN, Chulam TC, Silva FO, et al., 2017. Clinicopathologic analysis of 14 cases of odontogenic myxoma and review of the literature. *J Clin Exp Dent*, 9(4):e560-e563.
https://doi.org/10.4317/jced.52953

Fujita S, Hideshima K, Ikeda T, 2006. Nestin expression in odontoblasts and odontogenic ectomesenchymal tissue of odontogenic tumours. *J Clin Pathol*, 59(3):240-245.
https://doi.org/10.1136/jcp.2004.025403

Gomes CC, Diniz MG, Duarte AP, et al., 2011. Molecular review of odontogenic myxoma. *Oral Oncol*, 47(5):325-328.
https://doi.org/10.1016/j.oraloncology.2011.03.006

Hao J, Bao XX, Jin B, et al., 2015. Ca^{2+} channel subunit α 1D promotes proliferation and migration of endometrial cancer cells mediated by 17β-estradiol *via* the G protein-coupled estrogen receptor. *FASEB J*, 29(7):2883-2893.
https://doi.org/10.1096/fj.14-265603

Haser GC, Su HK, Hernandez-Prera JC, et al., 2016. Pediatric odontogenic fibromyxoma of the mandible: case report and review of the literature. *Head Neck*, 38(1):E25-E28.
https://doi.org/10.1002/hed.24090

Kauke M, Safi AF, Kreppel M, et al., 2018. Size distribution and clinicoradiological signs of aggressiveness in odontogenic myxoma-three-dimensional analysis and systematic review. *Dentomaxillofac Radiol*, 47(2):20170262.
https://doi.org/10.1259/dmfr.20170262

Kawase-Koga Y, Saijo H, Hoshi K, et al., 2014. Surgical management of odontogenic myxoma: a case report and review of the literature. *BMC Res Notes*, 7:214.
https://doi.org/10.1186/1756-0500-7-214

Kechin A, Boyarskikh U, Kel A, et al., 2017. CutPrimers: a new tool for accurate cutting of primers from reads of targeted next generation sequencing. *J Comput Biol*, 24(11):1138-1143.
https://doi.org/10.1089/cmb.2017.0096

Langmead B, Salzberg SL, 2012. Fast gapped-read alignment with Bowtie 2. *Nat Methods*, 9(4):357-359.
https://doi.org/10.1038/nmeth.1923

Lauer S, Gresham D, 2019. An evolving view of copy number variants. *Curr Genet*, 65(6):1287-1295.
https://doi.org/10.1007/s00294-019-00980-0

Legrand G, Humez S, Slomianny C, et al., 2001. Ca^{2+} pools and cell growth: evidence for sarcoendoplasmic Ca^{2+}-ATPases 2B involvement in human prostate cancer cell growth control. *J Biol Chem*, 276(50):47608-47614.
https://doi.org/10.1074/jbc.M107011200

Li TJ, Sun LS, Luo HY, 2006. Odontogenic myxoma: a clinicopathologic study of 25 cases. *Arch Pathol Lab Med*, 130(12):1799-1806.
https://doi.org/10.5858/2006-130-1799-omacso

Li XT, Liu L, Zhang JY, et al., 2021. Improvement in the risk assessment of oral leukoplakia through morphology-related copy number analysis. *Sci China Life Sci*, 64(9):1379-1391.
https://doi.org/10.1007/s11427-021-1965-x

Lyu J, Su Q, Liu JH, et al., 2022. Functional characterization of *piggyBac*-like elements from *Nilaparvata lugens* (Stål) (Hemiptera: Delphacidae). *J Zhejiang Univ-Sci B (Biomed & Biotechnol)*, 23(6):515-527.
https://doi.org/10.1631/jzus.B2101090

Ma M, Liu L, Shi RR, et al., 2021. Copy number alteration profiling facilitates differential diagnosis between ossifying fibroma and fibrous dysplasia of the jaws. *Int J Oral Sci*, 13:21.
https://doi.org/10.1038/s41368-021-00127-3

Maleszewski JJ, Larsen BT, Kip NS, et al., 2014. PRKAR1A in the development of cardiac myxoma: a study of 110 cases including isolated and syndromic tumors. *Am J Surg Pathol*, 38(8):1079-1087.
https://doi.org/10.1097/pas.0000000000000202

Mete O, Wenig BM, 2022. Update from the 5th edition of the World Health Organization Classification of Head and Neck Tumors: overview of the 2022 WHO classification of head and neck neuroendocrine neoplasms. *Head Neck Pathol*, 16(1):123-142.
https://doi.org/10.1007/s12105-022-01435-8

Mikhail FM, 2014. Copy number variations and human genetic disease. *Curr Opin Pediatr*, 26(6):646-652.
https://doi.org/10.1097/mop.0000000000000142

Pahl S, Henn W, Binger T, et al., 2000. Malignant odontogenic myxoma of the maxilla: case with cytogenetic confirmation. *J Laryngol Otol*, 114(7):533-535.
https://doi.org/10.1258/0022215001906075

Regezi JA, Sciubba J, Jordan RCK, 2015. Oral Pathology: Clinical Pathologic Correlations, 7th Ed. Elsevier, St. Louis, USA.

Samuel SM, Varghese E, Varghese S, et al., 2018. Challenges and perspectives in the treatment of diabetes associated breast cancer. *Cancer Treat Rev*, 70:98-111.
https://doi.org/10.1016/j.ctrv.2018.08.004

Santos JN, Sousa Neto ES, França JA, et al., 2017. Next-generation sequencing of oncogenes and tumor suppressor genes in odontogenic myxomas. *J Oral Pathol Med*, 46(10):1036-1039.
https://doi.org/10.1111/jop.12598

Stranger BE, Forrest MS, Dunning M, et al., 2007. Relative impact of nucleotide and copy number variation on gene expression phenotypes. *Science*, 315(5813):848-853.
https://doi.org/10.1126/science.1136678

Suarez PA, Batsakis JG, El-Naggar AK, 1996. Don't confuse dental soft tissues with odontogenic tumors. *Ann Otol Rhinol Laryngol*, 105(6):490-494.
https://doi.org/10.1177/000348949610500615

Tang YC, Amon A, 2013. Gene copy-number alterations: a cost-benefit analysis. *Cell*, 152(3):394-405.
https://doi.org/10.1016/j.cell.2012.11.043

Thoma KH, Goldman HM, 1947. Central myxoma of the jaw. *Am J Orthod Oral Surg*, 33(7):B532-B540.
https://doi.org/10.1016/0096-6347(47)90315-3

Williams JA, Hou YF, Ni HM, et al., 2013. Role of intracellular calcium in proteasome inhibitor-induced endoplasmic reticulum stress, autophagy, and cell death. *Pharm Res*, 30(9):2279-2289.
https://doi.org/10.1007/s11095-013-1139-8

Zhan D, Tanavalee A, Tantavisut S, et al., 2020. Relationships between blood leukocyte mitochondrial DNA copy

number and inflammatory cytokines in knee osteoarthritis. *J Zhejiang Univ-Sci B (Biomed & Biotechnol)*, 21(1):42-52. https://doi.org/10.1631/jzus.B1900352

Zhong WW, Wang DJ, Yao B, et al., 2021. Integrative analysis of prognostic long non-coding RNAs with copy number variation in bladder cancer. *J Zhejiang Univ-Sci B (Biomed & Biotechnol)*, 22(8):664-681. https://doi.org/10.1631/jzus.B2000494

Supplementary information

Tables S1–S5; Fig. S1